



Synthesis and characterization of photoactive azobenzene-based chromophores containing a bulky cholesteryl moiety

Po-Chih Yang^{a,*}, Ya-Ling Lu^b, Chung-Yuan Li^a

^a Department of Chemical Engineering and Materials Science, Yuan Ze University, Chung-Li 32003, Taiwan

^b Department of Applied Chemistry, Chaoyang University of Technology, Taichung 41349, Taiwan

ARTICLE INFO

Article history:

Received 12 August 2011

Received in revised form 3 January 2012

Accepted 13 February 2012

Available online 22 February 2012

Keywords:

Azobenzene

Photochemistry

Synthesis

UV–vis spectroscopy

Isomerization

ABSTRACT

This study describes the synthesis of a series of azobenzene-based chromophores bearing pendent bulky cholesteryl groups, using esterification reactions. The chromophores were composed of liquid crystalline mesophases with six or eleven methylene segments as spacers, and with electron-donating ($-\text{OCH}_3$) and electron-withdrawing ($-\text{NO}_2$) terminal groups. The target compounds were characterized by nuclear magnetic resonance spectroscopy, differential scanning calorimetry, polarizing optical microscopy, absorption, and photoluminescence spectroscopies. All the azobenzene derivatives with six or eleven methylene segments revealed chiral nematic phases. We investigated the effects of these photochromic compounds' structures on E/Z photoisomerization under UV irradiation. Chromophores containing the electron-withdrawing nitro-group ($-\text{NO}_2$) underwent a faster rate of Z to E isomerization in darkness than the electron-donating ($-\text{OCH}_3$) groups did; the isomerization process proceeded via a rotation mechanism. Self-assembled aggregates of **C6** solution exhibited enhanced fluorescence in THF/water mixtures at 10% water fraction.

© 2012 Elsevier B.V. All rights reserved.

1. Introduction

Liquid crystalline compounds (LCs) have been receiving increasing attention in the manipulation of optimized high-efficiency electro-optic devices because of their ability to self-assemble, their fluidity, and facile defect-free orientation under certain conditions [1,2]. The development of photosensitive media employing LCs for data recording, optical storage, and reproduction is one of the most rapidly developing areas in the physical chemistry area of low molecular mass and polymer LCs [3–6]. Cholesteric LCs incorporating photoisomerizable mesogenic fragments such as azobenzene [7,8] and stilbene [9,10], that can reverse their configurations when irradiated with light at various wavelengths, can be used to provide a motor function for contractions in photoresponsive materials [11]. Several groups have reported the preparation and applications of photoresponsive materials composed of fast photochemical segments [12–14]. Azobenzene-containing chromophores undergo isomerization from the E-isomer to the Z-form under irradiation by light, whereas the Z-isomer may return to the E form by either photochemical or thermal stimuli [15].

Fluorescent organic nanoparticles have also attracted considerable research attention because of their potential applications, including fluorescent biological labels [16], optical sensors [17],

light-emitting diodes [18], and photovoltaic cells [19]. Because of their unique properties that originate from quantum effects, fluorescent organic nanoparticles have significant potential, due to the wide variety of organic synthesis and nanocomposite preparation methods available. Systematic investigations into fluorescent organic nanoparticles began after Nakanishi and co-workers [20], reported that phthalocyanine and perylene nanoparticles exhibit different and size-dependent fluorescent properties from those of their bulk samples. Generally, the fluorescence quantum yields of organic chromophores decrease in the solid but exhibit high fluorescence quantum yields in solution. This occurs because of aggregation in the solid state, and mainly arises from intermolecular vibronic interactions, which induce non-radiative deactivation processes such as excitonic coupling, excimer formation, and excitation energy migration to impurity traps [21], resulting in decrease in fluorescence efficiency. However, a few cases of enhanced emission in the solid states of specific organic fluorophores, such as arylolefinyl compounds, pentaphenylsiloles, and poly(phenyleneethynylene) compounds, have been reported and interpreted as the intra- and inter-molecular effects exerted by fluorophore aggregation [22–24]. Thus, an aggregation-induced fluorescence enhancement was proposed [23]. Intermolecular effects by aggregation influence the fluorescence changes in π -conjugated organic chromophores. Effects on fluorescence changes by intermolecular interactions are correlated with the aggregation morphology such as H-type or J-type aggregation [21].

* Corresponding author. Tel.: +886 3 4638800; fax: +886 3 4559373.

E-mail address: pcyang@saturn.yzu.edu.tw (P.-C. Yang).

Unsubstituted azobenzenes show extremely little fluorescence with a small quantum yield of approximately 2.53×10^{-5} [25]. A few azobenzene derivatives in rigid matrices at low temperature, ortho-metalated azobenzenes, and self-assembled aggregates of azobenzene derivatives exhibit fluorescence [26–28]. Han et al. [29] reported increasing fluorescence quantum yields of UV-exposed azobenzene molecules with increasing electron-donating abilities of the substituents. Han et al. attributed this unusual fluorescence enhancement to the light-driven self-assembly of Z-isomers with significant lifetime and large dipole moment.

In our previous report [30], we demonstrated that self-assembled azobenzenes Z-isomers, incorporating the diacetylene group ($-\text{C}\equiv\text{C}-\text{C}\equiv\text{C}-$), exhibit fluorescence enhancement upon UV irradiation; this fluorescence originates from the formation of Z-isomer aggregates. Our system, based on configuration changes of azobenzene-based chromophores, exhibits simple photochemistry and offers ease of chemical modification. The current study examines the effect of terminal groups and spacer length of chromophore structure on photoreactivity and mesomorphic properties. We also investigate the solvent dependence of azobenzene aggregates' fluorescence enhancement. The effect of the structure of these photochromic compounds on E/Z photoisomerization under UV irradiation is discussed in detail.

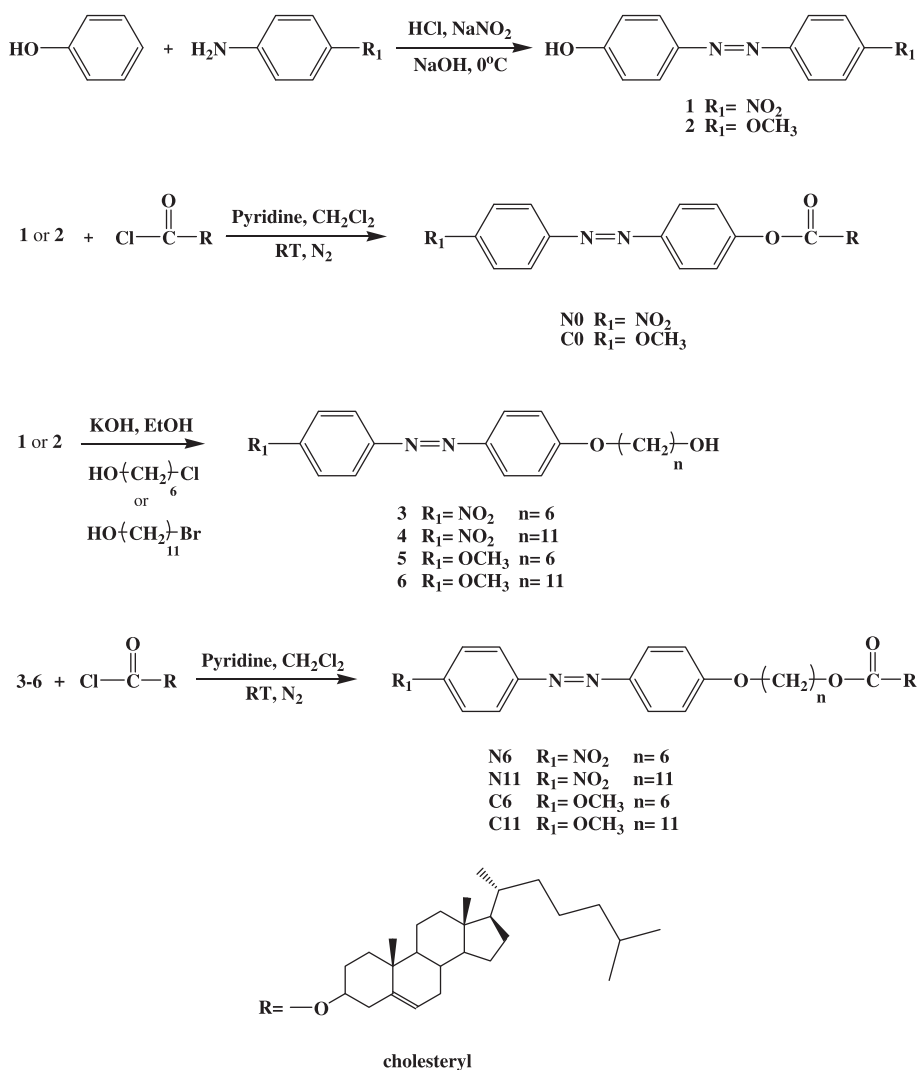
2. Experimental

2.1. Materials

Synthetic routes for the target photochromic compounds are shown in Scheme 1. The intermediates, 4-hydroxy-4'-nitro-azobenzene (**1**) and 4-hydroxy-4'-methoxy-azobenzene (**2**), 1-hydroxy-6-(4-nitro-azobenzene-4'-oxy) hexane (**3**), 1-hydroxy-11-(4-nitro-azobenzene-4'-oxy) undecane (**4**), 1-hydroxy-6-(4-methoxy-azobenzene-4'-oxy) hexane (**5**), 1-hydroxy-11-(4-methoxy-azobenzene-4'-oxy) undecane (**6**), and the target photochromic compounds were synthesized following the processes reported in the literature [31] and our previous reports [32,33]. All organic solvents and reagents were purchased from Acros, Alfa, and Aldrich Chemical Co. and used without further purification. Dichloromethane (CH_2Cl_2) was distilled over calcium hydride under argon immediately before use.

2.2. Measurements

All new compounds were identified by NMR, FT-IR spectra, and elemental analyses (EAs). ^1H NMR (400 MHz) and ^{13}C NMR (100.6 MHz) spectra were recorded on a Bruker AMX-400 FT-NMR, and chemical shifts were reported in ppm using tetramethyl-



Scheme 1. Synthetic routes of azobenzene-based chromophores.

silane (TMS) as an internal standard. FTIR spectra were measured as KBr disk using a Jasco VALOR III FTIR spectrometer; 32 scans were collected at a resolution of 1 cm^{-1} . Elemental analyses were carried out on a Heraeus CHN—O rapid elemental analyzer. Optical rotations were measured at $30\text{ }^{\circ}\text{C}$ in CHCl_3 using a Jasco DIP-370 polarimeter at the sodium D-line ($\lambda = 589\text{ nm}$) with a precision of $\pm 0.001^{\circ}$. The measurements were performed using 1% solutions of substances in CHCl_3 . UV/visible absorption spectra were measured using a Jasco V-550 spectrophotometer and photoluminescence (PL) spectra were obtained using a Jasco FP-750 fluorescence spectrophotometer. Fluorescence quantum yields of compounds in chloroform using 9,10-diphenylanthracene ($\lambda_{\text{ex}} = 350\text{ nm}$) as the standard were estimated at room temperature by the dilution method ($1 \times 10^{-7}\text{ M}$, assuming a quantum efficiency of unity) [34]. Thermal analysis was performed using a differential scanning calorimeter (Perkin Elmer DSC 7) at a scanning rate of 10 K min^{-1} under nitrogen atmosphere. The mesophase transitions were investigated by an Olympus BH-2 polarizing light microscope (POM) equipped with a Mettler FP-82 hot stage and a heating rate of 10 K min^{-1} . UV light (365 nm; Model UVG-54, UVP) with an intensity of 0.6 mW was used as a pumping light to induce photoisomerization of chiral compounds with N=N bonds in CHCl_3 solutions.

2.3. Synthesis of photochromic compounds (Scheme 1)

2.3.1. Synthesis of (–)-cholesteryl (4-nitro-azobenzene-4'-oxy) carboxylate, **N0**

4-Hydroxy-4'-nitro-azobenzene (**1**) (2.0 g, 8.22 mmol), pyridine (1.63 g, 20.61 mmol) and dry dichloromethane (50 ml) were put inside of a 150 ml two-necked flask equipped with a magnetic stirrer. Then cholesteryl chloroformate (7.38 g, 16.44 mmol) was added dropwise under vigorous stirring to the resulting solution under nitrogen atmosphere. After the reaction mixture was stirred under nitrogen atmosphere for 12 h at $30\text{ }^{\circ}\text{C}$, the solution was poured into water and extracted with chloroform. The organic layer was washed several times with water, dried over anhydrous MgSO_4 , and evaporated to dryness. The crude product was purified by column chromatography (silica gel, $\text{CH}_2\text{Cl}_2/n\text{-hexane} = 1/1$).

Yield: 76.5%. $T_m = 219.5\text{ }^{\circ}\text{C}$. $[\alpha]_D = -5.7^{\circ}$. FT-IR (KBr, $\nu_{\text{max}}/\text{cm}^{-1}$): 2941, 2868 (CH_2), 1763 ($\text{C}=\text{O}$), 1608, 1498 (CC in Ar), 1252 (COC), 1346 (NO_2). $^1\text{H NMR}$ (CDCl_3 , δ in ppm): 0.62 (s, 3H, CH_3), 0.79–1.02 (m, 12H, CH_3), 1.05–2.45 (m, 28H, CH_2), 4.52–4.57 (m, 1H, OCH in chol.), 5.36 (m, 1H, CHCH_2 in chol.), 7.32–7.34 (d, $J = 8.78\text{ Hz}$, 2H, aromatic), 7.93–7.95 (d, $J = 8.80\text{ Hz}$, 2H, aromatic, $-\text{ArN}=\text{NAr}-$), 7.96–7.98 (d, $J = 8.72\text{ Hz}$, 2H, aromatic, $-\text{ArN}=\text{NAr}-$), 8.31–8.33 (d, $J = 8.86\text{ Hz}$, 2H, aromatic, ortho to NO_2). $^{13}\text{C NMR}$ (100.6 MHz, CDCl_3): 12.0, 18.8, 19.3, 22.4, 22.4 (CH_3); 21.3, 24.2, 24.5, 27.7, 32.2, 32.5, 36.6, 38.0, 39.7, 39.8, 40.0 (CH_2); 42.4 (quaternary); 28.2, 31.7, 36.0, 50.3, 56.6, 56.2, 76.1 (CH); 122.6, 138.6 (vinylic); 120.2, 125.1, 125.8, 126.7 (aromatic); 147.6, 153.3, 155.3, 155.4 (aromatic quaternary); 153.9 ($\text{C}=\text{O}$). Anal. Calcd. (%) for $\text{C}_{40}\text{H}_{53}\text{N}_3\text{O}_5$: C, 73.19; H, 8.08; N, 6.40. Found: C, 73.06; H, 8.12; N, 6.45.

2.3.2. Synthesis of (–)-cholesteryl (4-methoxy-azobenzene-4'-oxy) carboxylate, **C0**

C0 was prepared by a procedure similar to that for **N0**, using 4-hydroxy-4'-methoxy-azobenzene (**2**) instead of 4-hydroxy-4'-nitro-azobenzene (**1**).

Yield: 61.8%. $T_m = 171.7\text{ }^{\circ}\text{C}$. $[\alpha]_D = -6.1^{\circ}$. FT-IR (KBr, $\nu_{\text{max}}/\text{cm}^{-1}$): 2940, 2863 (CH_2), 1760 ($\text{C}=\text{O}$), 1579, 1481 (CC in Ar), 1248 (COC). $^1\text{H NMR}$ (CDCl_3 , δ in ppm): 0.69 (s, 3H, CH_3), 0.86–1.05 (m, 12H, CH_3), 1.08–2.52 (m, 28H, CH_2), 3.88 (s, 3H, OCH_3), 4.57–4.66 (m, 1H, OCH in chol.), 5.43 (m, 1H, CHCH_2 in chol.), 6.99–7.02 (d, $J = 8.82\text{ Hz}$, 2H, aromatic), 7.31–7.34 (d, $J = 8.60\text{ Hz}$, 2H, aromatic),

7.88–7.90 (d, $J = 8.52\text{ Hz}$, 2H, aromatic), 7.90–7.92 (d, $J = 8.64\text{ Hz}$, 2H, aromatic). $^{13}\text{C NMR}$ (100.6 MHz, CDCl_3): 11.9, 18.8, 19.2, 22.4, 22.4 (CH_3); 21.2, 24.2, 24.5, 27.7, 32.2, 32.4, 36.7, 38.0, 39.8, 39.8, 40.0 (CH_2); 55.4 (OCH_3); 42.4 (quaternary); 28.1, 31.7, 36.0, 50.4, 56.6, 57.0, 75.1 (CH); 122.5, 138.7 (vinylic); 113.3, 120.3, 124.8, 126.8 (aromatic); 146.3, 149.2, 155.1, 166.8 (aromatic quaternary); 153.8 ($\text{C}=\text{O}$). Anal. Calcd. (%) for $\text{C}_{41}\text{H}_{56}\text{N}_2\text{O}_4$: C, 76.77; H, 8.74; N, 4.37. Found: C, 76.82; H, 8.75; N, 4.39.

2.3.3. Synthesis of (–)-cholesteryl 6-(4-nitro-azobenzene-4'-oxy) hexyl carbonate, **N6**

N6 was prepared by a procedure similar to that for **N0**, using 1-hydroxy-6-(4-nitro-azobenzene-4'-oxy) hexane (**3**) instead of 4-hydroxy-4'-nitro-azobenzene (**1**).

Yield: 76.5%. $K 138.7\text{ }^{\circ}\text{C N}^* 189.1\text{ }^{\circ}\text{C I}$ (heating). $[\alpha]_D = -4.4^{\circ}$. FT-IR (KBr, $\nu_{\text{max}}/\text{cm}^{-1}$): 2942, 2851 (CH_2), 1742 ($\text{C}=\text{O}$), 1603, 1471 (CC in Ar), 1257 (COC), 1344 (NO_2). $^1\text{H NMR}$ (CDCl_3 , δ in ppm): 0.67 (s, 3H, CH_3), 0.86–1.00 (m, 12H, CH_3), 1.05–2.41 (m, 28H, CH_2), 4.06 (t, $J = 6.35\text{ Hz}$, 2H, $-\text{OCH}_2-$), 4.14 (t, $J = 6.50\text{ Hz}$, 2H, $-\text{OCH}_2-$), 4.45–4.49 (m, 1H, OCH in chol.), 5.38–5.39 (m, 1H, CHCH_2 in chol.), 7.00–7.03 (d, $J = 8.80\text{ Hz}$, 2H, aromatic), 7.94–7.96 (d, $J = 9.40\text{ Hz}$, 2H, aromatic, $-\text{ArN}=\text{NAr}-$), 7.97–7.99 (d, $J = 9.30\text{ Hz}$, 2H, aromatic, $-\text{ArN}=\text{NAr}-$), 8.35–8.37 (d, $J = 8.80\text{ Hz}$, 2H, aromatic, ortho to NO_2). $^{13}\text{C NMR}$ (100.6 MHz, CDCl_3): 11.8, 18.7, 19.2, 22.5, 22.8 (CH_3); 21.0, 23.8, 24.3, 25.7, 27.7, 28.6, 29.0, 31.9, 36.2, 36.5, 38.1, 39.5, 39.7 (CH_2); 67.6, 68.2 (OCH_2); 42.3 (quaternary); 28.0, 31.8, 35.8, 50.0, 56.1, 56.7, 77.7 (CH); 122.9, 139.4 (vinylic); 114.9, 123.1, 124.7, 125.6 (aromatic); 146.8, 148.2, 154.7, 162.8 (aromatic quaternary); 156.1 ($\text{C}=\text{O}$). Anal. Calcd. (%) for $\text{C}_{46}\text{H}_{65}\text{N}_3\text{O}_6$: C, 73.01; H, 8.60; N, 5.56. Found: C, 72.98; H, 8.56; N, 5.57.

2.3.4. Synthesis of (–)-cholesteryl 6-(4-nitro-azobenzene-4'-oxy) undecyl carbonate, **N11**

N11 was prepared by a procedure similar to that for **N0**, using 1-hydroxy-11-(4-nitro-azobenzene-4'-oxy) undecane (**4**) instead of 4-hydroxy-4'-nitro-azobenzene (**1**).

Yield: 66.2%. $K 123.3\text{ }^{\circ}\text{C N}^* 162.9\text{ }^{\circ}\text{C I}$ (heating). $[\alpha]_D = -5.2^{\circ}$. FT-IR (KBr, $\nu_{\text{max}}/\text{cm}^{-1}$): 2934, 2853 (CH_2), 1733 ($\text{C}=\text{O}$), 1606, 1478 (CC in Ar), 1254 (COC), 1344 (NO_2). $^1\text{H NMR}$ (CDCl_3 , δ in ppm): 0.60 (s, 3H, CH_3), 0.78–0.93 (m, 12H, CH_3), 1.00–2.33 (m, 28H, CH_2), 3.99 (t, $J = 6.56\text{ Hz}$, 2H, $-\text{OCH}_2-$), 4.04 (t, $J = 6.68\text{ Hz}$, 2H, $-\text{OCH}_2-$), 4.37–4.43 (m, 1H, OCH in chol.), 5.32 (m, 1H, CHCH_2 in chol.), 6.95–6.97 (d, $J = 8.92\text{ Hz}$, 2H, aromatic), 7.88–7.90 (d, $J = 8.28\text{ Hz}$, 2H, aromatic, $-\text{ArN}=\text{NAr}-$), 7.90–7.92 (d, $J = 8.48\text{ Hz}$, 2H, aromatic, $-\text{ArN}=\text{NAr}-$), 8.28–8.30 (d, $J = 8.88\text{ Hz}$, 2H, aromatic, ortho to NO_2). $^{13}\text{C NMR}$ (100.6 MHz, CDCl_3): 11.7, 18.5, 19.2, 22.5, 22.6 (CH_3); 21.2, 24.2, 24.5, 25.9, 28.3, 28.6, 28.6, 28.6, 28.7, 28.9, 29.0, 29.1, 31.7, 32.2, 36.1, 36.5, 37.9, 39.4, 39.7 (CH_2); 67.5, 68.2 (OCH_2); 42.3 (quaternary); 27.8, 31.8, 35.4, 49.8, 56.0, 56.3, 77.0 (CH); 122.6, 138.2 (vinylic); 114.2, 123.0, 124.1, 125.3 (aromatic); 146.8, 148.1, 154.1, 162.4 (aromatic quaternary); 155.5 ($\text{C}=\text{O}$). Anal. Calcd. (%) for $\text{C}_{51}\text{H}_{75}\text{N}_3\text{O}_6$: C, 74.08; H, 9.11; N, 5.08. Found: C, 74.04; H, 9.15; N, 5.13.

2.3.5. Synthesis of (–)-cholesteryl 6-(4-methoxy-azobenzene-4'-oxy) hexyl carbonate, **C6**

C6 was prepared by a procedure similar to that for **N0**, using 1-hydroxy-6-(4-methoxy-azobenzene-4'-oxy) hexane (**5**) instead of 4-hydroxy-4'-nitro-azobenzene (**1**).

Yield: 60.5%. $K 160.0\text{ }^{\circ}\text{C N}^* 185.4\text{ }^{\circ}\text{C I}$ (heating). $[\alpha]_D = -7.2^{\circ}$. FT-IR (KBr, $\nu_{\text{max}}/\text{cm}^{-1}$): 2940, 2858 (CH_2), 1744 ($\text{C}=\text{O}$), 1589, 1471 (CC in Ar), 1274 (COC). $^1\text{H NMR}$ (CDCl_3 , δ in ppm): 0.66 (s, 3H, CH_3), 0.84–1.00 (m, 12H, CH_3), 1.10–2.48 (m, 28H, CH_2), 3.88 (s, 3H, OCH_3), 4.03 (t, $J = 6.56\text{ Hz}$, 2H, $-\text{OCH}_2-$), 4.14 (t, $J = 6.73\text{ Hz}$, 2H, $-\text{OCH}_2-$), 4.44–4.49 (m, 1H, OCH in chol.), 5.40 (m, 1H, CHCH_2 in chol.),

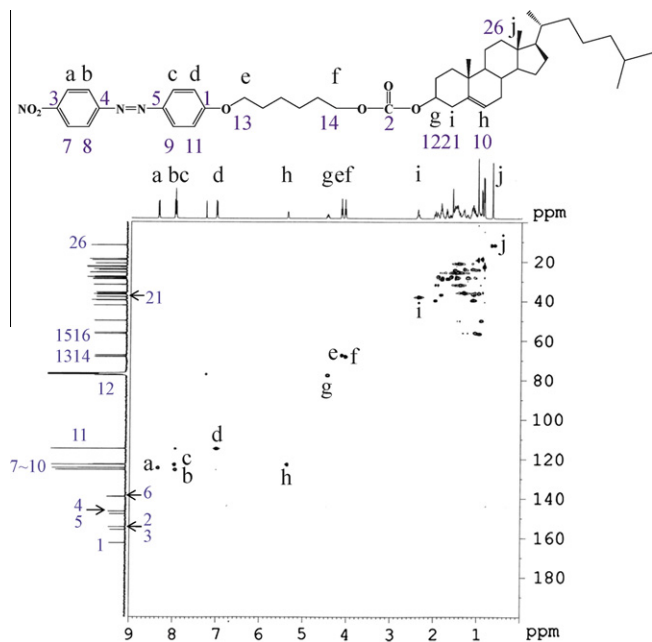


Fig. 1. C–H HMQC NMR spectrum of **N6**.

6.95–6.98 (d, $J = 8.80$ Hz, 2H, aromatic), 6.99–7.02 (d, $J = 8.64$ Hz, 2H, aromatic), 7.83–7.85 (d, $J = 8.50$ Hz, 2H, aromatic), 7.88–7.90 (d, $J = 8.64$ Hz, 2H, aromatic). ^{13}C NMR (100.6 MHz, CDCl_3): 11.9, 18.8, 19.2, 22.4, 22.4 (CH_3); 21.2, 24.3, 24.5, 25.6, 27.2, 28.9, 28.9, 29.2, 32.2, 32.4, 36.6, 39.1, 39.8, 39.9, 40.0 (CH_2); 55.5 (OCH_3); 67.4, 68.1 (OCH_2); 42.4 (quaternary); 28.1, 31.8, 36.1, 50.4, 56.5, 56.9, 75.1 (CH); 122.5, 138.7 (vinylic); 110.4, 113.3, 123.4, 124.9 (aromatic); 146.3, 146.3, 166.5, 166.9 (aromatic quaternary); 155.7 ($\text{C}=\text{O}$). Anal. Calcd. (%) for $\text{C}_{47}\text{H}_{68}\text{N}_2\text{O}_5$: C, 76.11; H, 9.18; N, 3.78. Found: C, 76.14; H, 9.23; N, 3.75.

2.3.6. Synthesis of (–)-cholesteryl 6-(4-methoxy-azobenzene-4'-oxy) undecyl carbonate, **C11**

C11 was prepared by a procedure similar to that for **N0**, using 1-hydroxy-11-(4-methoxy-azobenzene-4'-oxy) undecane (**6**) instead of 4-hydroxy-4'-nitro-azobenzene (**1**).

Table 1
Thermal properties of azobenzene-based chromophores.

No.	R^a	$[\alpha]_D^{20}$ ^b	Transition temperature ($^{\circ}\text{C}$) ^c (corresponding enthalpy changes (J g^{-1}))	ΔT_h^d ΔT_c^d
N0	NO_2	–5.7	K 219.5 (55.1) I I 194.0 (–46.5) K	– –
N6	NO_2	–4.4	K 138.7 (67.2) N* 189.1 (4.1) I I 187.6 (–3.9) N* 108.8 (–43.0) K	50.4 78.8
N11	NO_2	–5.2	K 123.2 (53.0) N* 162.9 (2.7) I I 161.0 (–2.9) N* 100.6 (–46.0) K	39.6 60.4
C0	OCH_3	–6.1	K 171.7 (58.2) I I 107.8 (–41.7) K	– –
C6	OCH_3	–7.2	K 160.0 (68.0) N* 185.4 (3.9) I I 183.1 (–3.9) N* 135.6 (–59.9) K	25.4 47.5
C11	OCH_3	–4.6	K 101.9 (44.8) N* 168.5 (3.0) I I 165.1 (–3.8) N* 86.9 (–34.1) K	66.6 78.2

^a Terminal groups of the synthesized compounds.

^b Specific rotation of compounds, $[\alpha]_D = \alpha/(l \times \rho)$; l is the path length in decimeters ($l = 1$ dm), and ρ is the density of the liquid in g/ml ; concentration: 0.1 g in 10 ml chloroform.

^c Phase transition temperature during second heating and first cooling scans at a rate of 10 K min^{-1} ; K, crystal; N*, chiral nematic (cholesteric); I, isotropic phase.

^d $\Delta T_h = T_{\text{iso}} - T_{\text{K} \rightarrow \text{N}^*}$ in heating cycle; $\Delta T_c = T_{\text{iso}} - T_{\text{K} \rightarrow \text{N}^*}$ in cooling cycle.

Yield: 60.4%. K 101.9 $^{\circ}\text{C}$ N* 168.5 $^{\circ}\text{C}$ I (heating). $[\alpha]_D = -4.6$. FT-IR (KBr, $\nu_{\text{max}}/\text{cm}^{-1}$): 2935, 2851 (CH_2), 1739 ($\text{C}=\text{O}$), 1584, 1476 (CC in Ar), 1276 (COC). ^1H NMR (CDCl_3 , δ in ppm): 0.60 (s, 3H, CH_3), 0.78–1.00 (m, 12H, CH_3), 1.02–2.33 (m, 28H, CH_2), 3.81 (s, 3H, OCH_3), 3.96 (t, $J = 6.54$ Hz, 2H, $-\text{OCH}_2-$), 4.04 (t, $J = 6.72$ Hz, 2H, $-\text{OCH}_2-$), 4.37–4.39 (m, 1H, OCH in chol.), 5.32 (m, 1H, CHCH_2

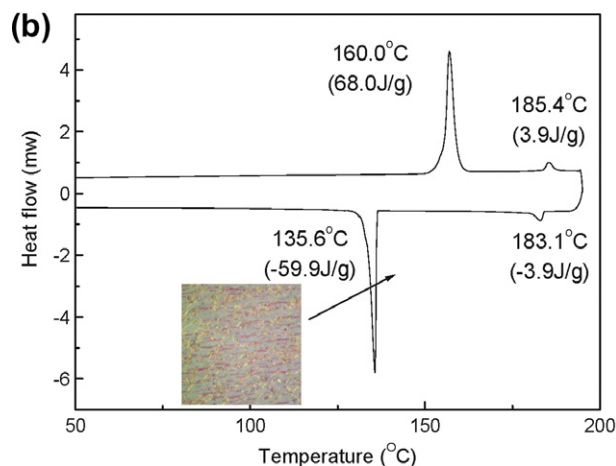
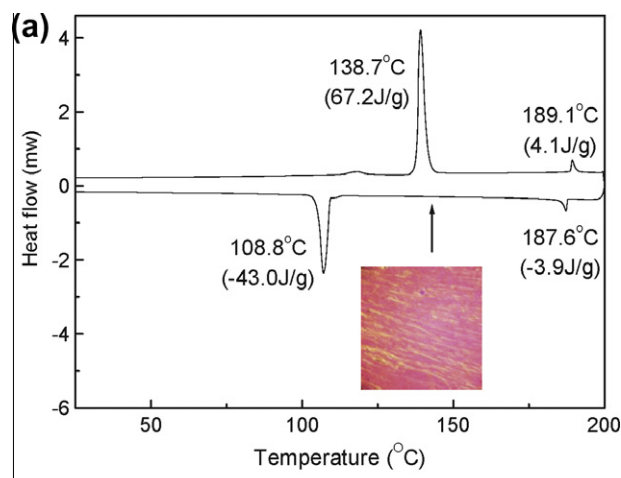


Fig. 2. DSC thermograms of (a) **N6** and (b) **C6**. Inset: polarizing microscopic textures at the corresponding state indicated in the figures ($100\times$ magnification).

Table 2
Optical properties of azobenzene-based chromophores.

No.	UV-vis λ_{max} (nm) ($\log \epsilon$) ^a	PL λ_{max} (nm) ^b	Φ_{PL} ^c	t_{365}^d	t_{dark}^e
N0	342 (4.36)	413, 437, 465 s	0.022	8 m	730 m
N6	380 (4.23)	413, 438, 466 s	0.035	1 m	60 m
N11	381 (4.21)	413, 437, 461 s	0.042	1 m	60 m
C0	349 (4.52)	415, 436	0.016	2 m	70 h
C6	359 (4.51)	414, 434	0.017	1 m	54 h
C11	359 (4.51)	416, 438	0.028	50 s	26 h

^a Maximum wavelength of the π – π^* transition of compounds in CHCl_3 solution; concentration: 1×10^{-5} M. Extinction coefficient ($\text{M}^{-1} \text{cm}^{-1}$) in the maxima absorption of UV-vis spectra.

^b The excitation wavelengths were the maxima absorption of UV-vis spectra (concentration: 1×10^{-5} M). Superscript s means the wavelength of the shoulder.

^c These values of quantum efficiency were measured using 9,10-diphenylanthracene as a standard (concentration: 1×10^{-7} M, assuming a quantum efficiency of unity).

^d Time to reach the photostationary state of UV irradiation (365 nm).

^e Time to reach the photostationary state in the dark after UV irradiation of 365 nm.

in chol.), 6.90–6.92 (d, $J=8.80$ Hz, 2H, aromatic), 6.92–6.94 (d, $J=8.66$ Hz, 2H, aromatic), 7.78–7.80 (d, $J=8.52$ Hz, 2H, aromatic), 7.80–7.82 (d, $J=8.66$ Hz, 2H, aromatic). ^{13}C NMR (100.6 MHz, CDCl_3): 11.9, 18.8, 19.2, 22.4, 22.5 (CH_3); 21.2, 24.2, 24.5, 25.9, 28.4, 28.5, 28.5, 28.6, 28.9, 28.9, 29.0, 29.1, 32.1, 32.4, 36.6, 39.1, 39.8, 39.8, 40.0 (CH_2); 55.4 (OCH_3); 67.4, 68.1 (OCH_2); 42.4 (quaternary); 28.2, 31.8, 36.0, 24.3, 50.3, 57.0, 75.2 (CH); 122.5, 138.7 (vinylic); 110.4, 113.3, 123.4, 124.9 (aromatic); 146.3, 146.4, 166.5, 166.9 (aromatic quaternary); 155.6 ($\text{C}=\text{O}$). Anal. Calcd. (%) for $\text{C}_{52}\text{H}_{78}\text{N}_2\text{O}_5$: C, 76.92; H, 9.62; N, 3.45. Found: C, 76.88; H, 9.65; N, 3.47.

3. Results and discussion

3.1. Synthesis and characterization

A series of azobenzene-based chromophores containing terminal electron-donating methoxy ($-\text{OCH}_3$) and electron-withdrawing nitro ($-\text{NO}_2$) moieties were prepared to investigate the effect of E/Z photoisomerization on the optical spectra under UV irradiation. Scheme 1 describes the route followed for the synthesis of these chromophores. The intermediates, bearing hydroxyl groups, and six or eleven methylene segments as spacers, **3–6**, were

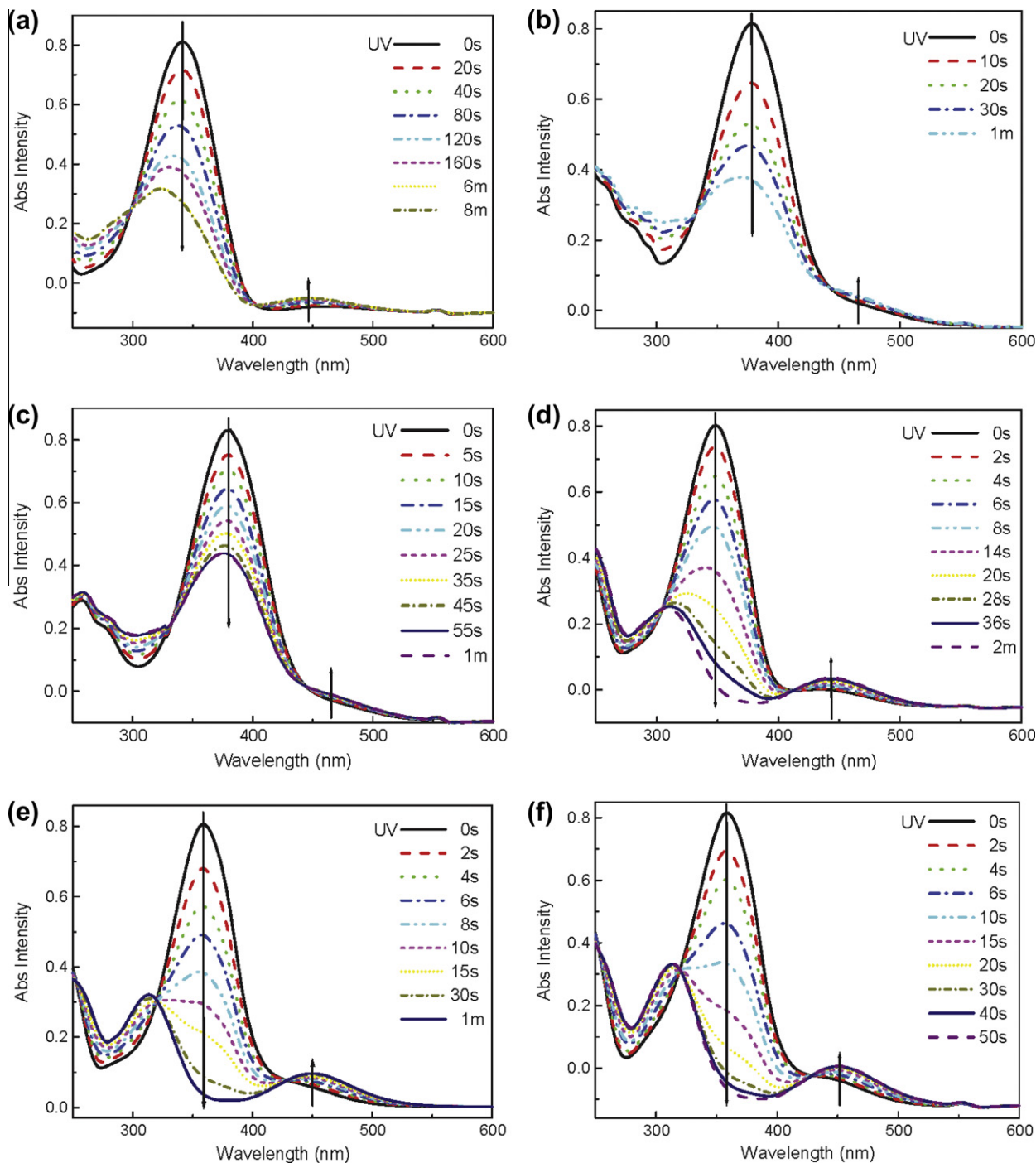


Fig. 3. UV-vis spectra before and after UV irradiation with 365 nm for (a) **N0**, (b) **N6**, (c) **N11**, (d) **C0**, (e) **C6**, and (f) **C11**.

synthesized using **1**, **2** and 6-chloro-1-hexanol, or 11-bromo-1-undecanol as reactants, in the presence of KOH in EtOH, under reflux. The six target chromophores were synthesized by esterification of **1–6** with cholesteryl chloroformate, using pyridine as a base, in dry dichloromethane solution at 30 °C under nitrogen atmosphere. Chemical structures and constitutional composition of the synthesized compounds were confirmed by elemental analysis, FTIR, and NMR spectroscopies. The ^1H NMR spectra of two representative compounds (**N6** and **C6**) in CDCl_3 are shown in Fig. SI-1a. In **N6**, the aromatic protons at H_a appear as a doublet at the most downfield position (8.35–8.37 ppm). Compared to **N6**, the aromatic protons H_c and H_d in **C6** (Fig. SI-1b) appear at higher field (6.95–7.02 ppm) than the other aromatic protons at H_a and H_b for **C6** do; this is because of the adjacent electron-donating ($-\text{OCH}_3$) terminal groups. ^1H and ^{13}C assignments of **N6** were confirmed by a combination of DEPT-135 (Fig. SI-2), and C–H HMQC (Fig. 1) methods, as were the assignments of **N0**, **C0**, **C6**, **N11** and **C11**. The proton resonances in the C–H HMQC spectrum show good correlation with the corresponding ^{13}C resonances. The molecular structures of the synthesized compounds were also supported by elemental analysis.

3.2. Thermal and liquid crystalline properties

Phase transition temperatures and the phases of the synthesized compounds are summarized in Table 1. The data listed in Table 1 show that the effect of molecular structure on melting temperature, mesomorphic properties, and even molecular arrangement of the chromophores was considerable. Chromophores **N0** and **C0**, without the presence of flexible spacer lengths do not show any LC mesophase. In general, LC mesophase must

contain suitable polarity and spacer length at the center and terminals. It appears that compounds lacking the long methylene chain as a flexible linkage stack via mesogenic side chains, and thus, there is an absence of mesophase in compounds **N0** and **C0**. However, **N6**, **N11**, **C6**, and **C11**, which all incorporate six or eleven methylene segments as spacers, exhibit mesomorphic phases. The four chromophores show enantiotropic mesophases, and reveal chiral nematic phases (N^* ; oily streaky texture), which we attributed to the introduction of a flexible spacer between the mesogenic core and the terminal groups to decouple side chain motions from the terminal groups in the mesophase, during heating and cooling cycles. The LC phases were confirmed using DSC analyses and were compared with polarizing optical microscopy (POM) textures, as reported in the literature [35].

Fig. 2 shows DSC thermograms and POM textures for **N6** and **C6** at a heating rate of 10 K min^{-1} . During the heating scan, **N6** melted, and a chiral nematic mesophase was observed between 138.7 and 189.1 °C before isotropization occurred. During the cooling scan, we observed an isotropic-to-chiral nematic phase transition at 187.6 °C and crystallization at 108.8 °C. **C6**, with an electron releasing methoxy ($-\text{OCH}_3$) segment, exhibited enantiotropic mesophase in the temperature ranges 160.0–185.4 °C, and 135.6–183.1 °C during heating and cooling cycles, respectively (Fig. 4b). In comparison, **N6** showed broader phase transition temperature ranges than **C6** did, suggesting that the electron-withdrawing nitro ($-\text{NO}_2$) moiety enhances the head-to-tail molecular interaction, because of the existence of strong nitro π – π interactions. However, introduction of the longer eleven methylene section as a spacer in **N11** might decrease head-to-tail molecular interactions, resulting in a reduction in phase transition temperature ranges. By contrast, chromophores **C6** and **C11** that incorporate terminal electron-

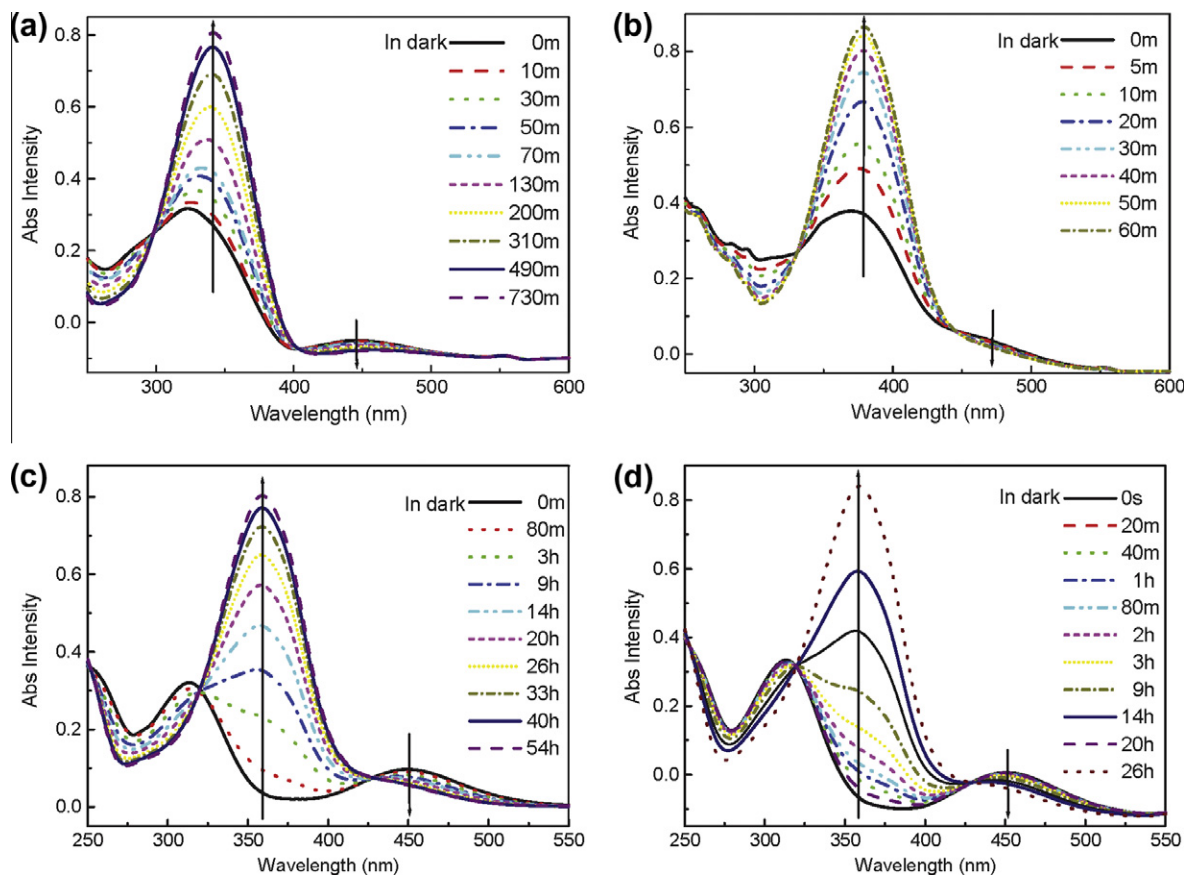


Fig. 4. Stability of UV-vis spectra of (a) **N0**, (b) **N6**, (c) **C6**, and (d) **C11** in the dark.

donating methoxy moieties, exhibit different behavior to that of **N6** and **N11**. Compound **C11** showed broader phase transition temperature ranges compared with those of **C6**. The results suggest that the rigidity of the mesogenic core, the flexible spacer length, and types of terminal unit have a large influence on intermolecular and dipole-induced dipole interactions, leading to the observed variation in phase transition temperatures. It also indicates that the terminal substituent is important in size and in the nature of its polarity. Consequently, the intermolecular interaction, dipole-induced dipole interactions might play an important role in determining the type of mesophase textures and influence the physical properties of the LC compounds [36]. Furthermore, as shown in Table 1, the enthalpy changes for the chiral nematic to isotropic phase transition in the range 2.7–4.1 J g⁻¹ were smaller than those of the chiral nematic to crystallization phase transition (around 34.1–68.0 J g⁻¹), consistent with the ordering of the molecular arrangement.

Right and left rotations of plane-polarized light passing through the compounds occurred, depending on the arrangement of ligands around the chiral center. In principle, the characteristic net vector of the rotation of plane-polarized light varies with polarity of the chiral molecules [37]. The specific rotation of cholesteryl chloroformate is -28°. As set out in Table 1, the specific rotations of chiral chromophores derived from cholesteryl chloroformate have negative values. Specifically, it was found that chirality could be a factor, which influences the physical properties of the compounds. Cleavage of the C–Cl bond and the binding of an azobenzene group significantly affect the chirality of these compounds. Our findings suggest that the specific rotation is influenced by the coherence of polarity changes due to chemical bonding during the esterification reaction.

3.3. Optical properties

We studied the E/Z isomerization of the azobenzene-based chromophores substituted with various terminal groups, to explore the photoreactivity of these compounds. Optical properties were investigated using UV-vis and PL spectroscopies. E-Z photoisomerization of chromophores was studied by UV absorption spectroscopy at 365 nm in CHCl₃. Table 2 summarizes the UV-vis absorption data for the photochromic compounds. These compounds exhibit strong UV-vis absorption bands at 342–381 nm, which we attribute to a π - π^* transition of the chromophore in the E-isomer. Weak absorption bands at approximately 440–450 nm resulted from an n - π^* transition in the E-isomer. The absorption maxima for **N6** and **N11**, which incorporate the electron-withdrawing nitro group, are located at approximately 380–381 nm, and are red-shifted (ca. 21–22 nm) relative to **C6** and **C11**, which incorporate the electron-donating methoxy group. Our results suggest that the electronic transition in **N6** and **N11** involves a migration of electron density from a donor group (-OR-) toward an acceptor group (-NO₂), leading to the bathochromic shifts seen for **N6** and **N11**. The UV-vis spectra in Fig. 3 shows the variation in shift for various UV irradiation times for all of our synthesized compounds. Fig. 4 illustrates the stability of four representative compounds in darkness. UV irradiation induces a decrease in the absorption intensity of the absorption maxima, and an increase in absorption at approximately 450 nm during irradiation. As shown in Fig. 3, an E-Z photostationary state was obtained for **N6** and **N11** within 1 min of irradiation. The observed variation in absorptions for the various compounds might result from the geometric change from the E-isomer to the Z-isomer of the azo compounds. The E-Z isomerization rate and time of photostationary state under UV irradiation were influenced by various potential energy profiles between E/Z isomers and dipolar transition state [31]. In darkness, **N6** and **N11** achieved thermal stability

for Z-E isomerization within 60 min, as shown in Fig. 4b and Table 2. Fig. 4c and d shows a steady state for Z-E isomerization after 54 h and 26 h for **C6** and **C11**, respectively, implying that **N6** and **N11**, which incorporate the nitro terminal group, use a rotation mechanism with low potential energy profile to achieve a faster rate of Z-E isomerization in darkness than **C6** and **C11** do [31].

As shown in Table 2 and Fig. 5, the fluorescence spectra of **N** and **C** series azobenzene-based compounds in CHCl₃ at ambient temperatures, exhibit emission maxima at approximately 413–438 nm. The **N** series fluorescence peaks include two well defined, and one shoulder at approximately 413, 437, and 465 nm; these might arise from the different vibrational-rotational levels of the excited states and ground electronic states. The PL quantum yields of photochromic compounds, estimated using 9,10-diphenylanthracene as reference, were at the range of 0.016–0.042.

3.4. Fluorescence enhancement effect on PL properties

In this study, we conducted fluorescence spectroscopy on azobenzene solutions to further investigate solvent effects on luminescence properties. The percentages of THF/water mentioned in the text refer to volume ratios of water. The solutions were left to equilibrate at room temperature for 30 min after preparation before carrying out further studies. Fig. 6 shows the UV-vis and PL spectra of **C6** in THF/water (good/non-solvent) mixtures with various volume ratios of water. In dilute THF solution, the azobenzene molecules were well-dissolved and isolated. **C6**

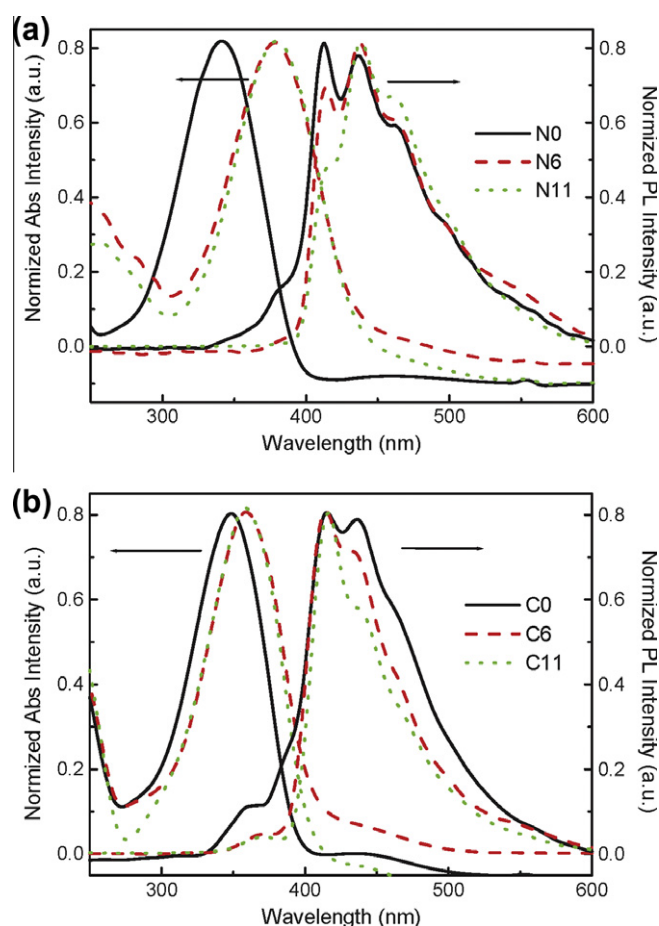


Fig. 5. Normalized UV-vis and PL spectra of (a) **N** and (b) **C** series compounds in chloroform.

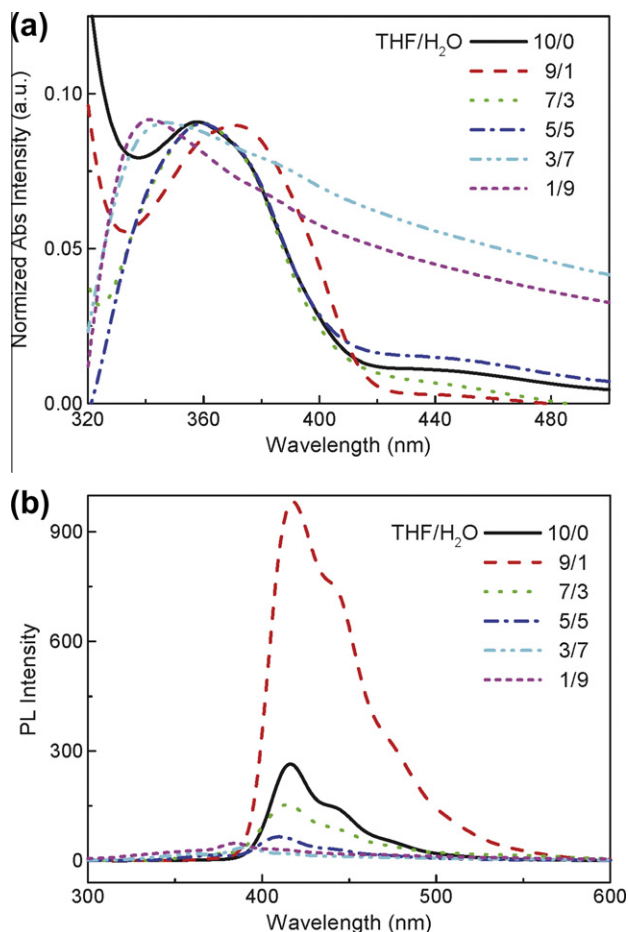


Fig. 6. Dependence of THF/water mixture on (a) UV-vis and (b) PL spectra of C6.

exhibited a typical azobenzene absorption spectrum with a weak $n-\pi^*$ transition at approximately 440–450 nm and an intense $\pi-\pi^*$ transition moment along the long-axis at 358 nm. Increase of water content in the solution (i.e. THF/water = 9/1) resulted in a red shift (ca. 14 nm) of the main absorption band centered at approximately 372 nm (Fig. 6a). This bathochromic effect might indicate that effective conjugation length of C6 is extended from the isolated twisted molecule to the planar one in nanoparticles. Aggregates were spontaneously formed upon adding non-solvent to the THF solution of C6. The bulky cholesteryl and polar carbonate groups in C6 might play important roles of restricting the parallel face-to-face intermolecular interactions in the aggregated state. Preventing parallel orientation of conjugated chromophores tends to favor J-aggregation with enhanced fluorescence emission instead of H-aggregation in the solid state. Extended conjugation and J-aggregation lead to the dramatic increase of the fluorescence intensity in 10% volume fractions of water addition of C6 nanoparticles as shown in Fig. 6b. However, with subsequent increase in water content (i.e. THF/water = 3/7 and 1/9), the blue shift of the absorption band was accompanied by a decrease in intensity. The solutions containing aggregates exhibited a blue shift due to the scattering of incident light. The original quantum yield of C6 in THF solution is low at 0.017. When the water fraction in the THF/water mixture reaches 10%, the quantum yield rises to 0.203, approximately 12 times greater than that in THF alone. The quantum yield increases significant upon adding up to 10% water, but decreases again at greater dilutions. This also indicates that fluorescence enhancement effect on C6 in 10% THF/water mixture might be due to

fluorophore aggregation. The enhanced fluorescence emission in azo nanoparticles might also result from the combined effects of aggregation-induced planarization and J-aggregation formation, which restrict parallel face-to-face intermolecular interactions and the formation of excimers in the aggregated state [38,39]. Enhanced fluorescence did not occur in N series solutions. The results are thus consistent with the substituent effects of azobenzene derivatives seen for fluorescence intensity, suggesting that the electron-donating group at the terminal position is important for intense emission [40]. A detailed investigation of PL solvent-dependence and scanning electron microscopy morphologies of azobenzene nanoparticles is now in progress.

4. Conclusions

We successfully synthesized and characterized six azobenzene-substituted chromophores. The optical properties of the photochromic compounds were evaluated using UV-vis and PL spectroscopies. All synthesized compounds bearing six or eleven methylene segments revealed chiral nematic phases, and exhibited an oily streaky texture. Introduction of the nitro-group in a terminal position resulted in increased Z to E isomerization rates in darkness. We have demonstrated that C6 azobenzene nanoparticles aggregate in THF/water solution at a 10% water fraction.

Acknowledgment

The authors are thankful for the National Science Council of the Republic of China (Taiwan) for its financial aid through project NSC 99-2113-M-115-001.

Appendix A. Supplementary material

Supplementary data associated with this article can be found, in the online version, at doi:10.1016/j.molstruc.2012.02.032.

References

- [1] M. O'Neill, S.M. Kelly, *Adv. Mater.* 15 (2003) 1135–1146.
- [2] A.J.J.M. van Breemen, P.T. Herwig, C.H.T. Chlon, J. Sweelssen, H.F. Schoo, M. Setayesh, W.M. Hardeman, C.A. Martin, D.M. de Leeuw, J.J.P. Valetton, C.W.M. Bastiaansen, D.J. Broer, A.R. Popa-Merticaru, S.C.J. Meskers, *J. Am. Chem. Soc.* 128 (2006) 2336–2345.
- [3] G. Schwarz, H.R. Kricheldorf, *J. Polym. Sci. Part A: Polym. Chem.* 34 (1996) 603–611.
- [4] S.H. Chen, H. Shi, B.M. Conger, J.C. Mastrangelo, T. Tsutsui, *Adv. Mater.* 8 (1996) 998–1001.
- [5] C.T. Chen, Y.T. Chou, *J. Am. Chem. Soc.* 122 (2000) 7662–7672.
- [6] Y. Wu, A. Kanazawa, T. Shiono, T. Ikeda, Q. Zhang, *Polymer* 40 (1999) 4787–4793.
- [7] A. Bobrovsky, V. Shibaev, *Polymer* 47 (2006) 4310–4317.
- [8] N. Tamaoki, S. Song, M. Moriyama, H. Matsuda, *Adv. Mater.* 12 (2000) 94–97.
- [9] R. Giménez, M. Millaruelo, M. Piñol, J.L. Serrano, A. Viñuales, R. Rosenhauer, T. Fischer, *J. Stumpe, Polymer* 46 (2005) 9230–9242.
- [10] R. Giménez, M. Piñol, J.L. Serrano, A.I. Viñuales, R. Rosenhauer, J. Stumpe, *Polymer* 47 (2006) 5707–5714.
- [11] Y. Wu, J. Mamiya, T. Shiono, T. Ikeda, Q. Zhang, *Macromolecules* 32 (1999) 8829–8835.
- [12] P.M. Hogan, A.R. Tajbakhsh, E.M. Terentjev, *Phys. Rev. E* 65 (2002) 041720.
- [13] Y. Yu, M. Nakato, T. Ikeda, *Nature* 425 (2003) 145.
- [14] M.H. Li, P. Keller, B. Li, X.G. Wang, M. Brunet, *Adv. Mater.* 15 (2003) 569–572.
- [15] N. Tamai, H. Miyasaka, *Chem. Rev.* 100 (2000) 1875–1890.
- [16] M. Bruchez, M. Moronne, P. Gin, S. Weiss, A.P. Alivisatos, *Science* (1998) 2013–2016.
- [17] A.N. Shipway, E. Katz, I. Willner, *ChemPhysChem* 1 (2000) 18–52.
- [18] A. Hagfeldt, M. Grätzel, *Chem. Rev.* 95 (1995) 49–68.
- [19] M.C. Schlamp, X. Peng, A.P. Alivisatos, *J. Appl. Phys.* 82 (1997) 5837–5842.
- [20] H. Kasai, H. Kamatani, Y. Yoshikawa, S. Okada, H. Oikawa, A. Watanabe, O. Ito, H. Nakanishi, *Chem. Lett.* (1997) 1181–1182.
- [21] J.B. Birks, *Photophysics of Aromatic Molecules*, Wiley-Interscience, London, 1970.
- [22] M. Levitus, K. Schmieder, H. Ricks, K.D. Shimizu, U.H.F. Bunz, M.A. Garcia-Garibay, *J. Am. Chem. Soc.* 123 (2001) 4259–4265.

- [23] J. Luo, Z. Xie, J.W.Y. Lam, L. Cheng, H. Chen, C. Qiu, H.S. Kwok, X. Zhan, Y. Liu, D. Zhu, B.Z. Tang, *Chem. Commun.* (2001) 1740–1741.
- [24] R. Deans, J. Kim, M.R. Machacek, T.M. Swager, *J. Am. Chem. Soc.* 122 (2000) 8565–8566.
- [25] H. Rau, *Angew. Chem. Int. Ed. Engl.* 12 (1973) 224–235.
- [26] M. Nepraš, S. Luňák Jr., R. Hrdina, J. Fabian, *Chem. Phys. Lett.* 159 (1989) 366–370.
- [27] Y. Wakatsuki, H. Yamazaki, P.A. Grutsch, M. Santhanam, C. Kotal, *J. Am. Chem. Soc.* 107 (1985) 8153–8159.
- [28] M. Han, M. Hara, *J. Am. Chem. Soc.* 127 (2005) 10951–10955.
- [29] M.R. Han, Y. Hirayama, M. Hara, *Chem. Mater.* 18 (2006) 2784–2786.
- [30] P.C. Yang, Y.H. Wang, H. Wu, *J. Appl. Polym. Sci.* 124 (2012) 4193–4205.
- [31] C.H. Ho, K.N. Yang, S.N. Lee, *J. Polym. Sci. Part A: Polym. Chem.* 39 (2001) 2296–2307.
- [32] J.H. Liu, P.C. Yang, *J. Appl. Polym. Sci.* 91 (2004) 3693–3704.
- [33] P.C. Yang, M.Z. Wu, J.H. Liu, *Polymer* 49 (2008) 2845–2856.
- [34] H.J. Son, W.S. Han, K.R. Wee, S.H. Lee, *J. Mater. Chem.* 19 (2009) 8964–8973.
- [35] I. Dierking, *Textures of Liquid Crystals*, Wiley-VCH, Weinheim, 2003.
- [36] K. Rameshbabu, P. Kannan, R. Velu, P. Ramamurthy, *Liq. Cryst.* 32 (2005) 823–832.
- [37] D.P. Shomaker, *Experimental Physical Chemistry*, McGraw-Hill, 1989. pp. 728–729.
- [38] D. Oelkrug, A. Tompert, J. Gierschner, H. Egelhaaf, M. Hanack, *J. Phys. Chem. B* 102 (1998) 1902–1907.
- [39] G. Narayan, N.S.S. Kumara, S. Paul, O. Srinivas, N. Jayaraman, S. Dasa, *J. Photochem. Photobiol. A: Chem.* 189 (2007) 405–413.
- [40] J. Yoshino, A. Furuta, T. Kambe, H. Itoi, N. Kano, T. Kawashima, Y. Ito, M. Asashima, *Chem. Eur. J.* 16 (2010) 5026–5035.